

A Transition Metal Containing Rotaxane in Motion: Electrochemically Induced Pirouetting of the Ring on the Threaded Dumbbell

Laurence Raehm, Jean-Marc Kern,* and Jean-Pierre Sauvage*[a]

Abstract: In this work we describe a rotaxane in which a new type of motion, pirouetting of the wheel around its axle, can be electrochemically triggered. The rotaxane was synthesized by using the three-dimensional effect of copper(i). It incorporates both a hetero-bis-coordinating ring (containing both 2,9-diphenyl-1,10-phenanthroline and 2,2':6',2''-terpyridine units) and a molecular string which contains only one 2,9-diphenyl-1,10-phenanthroline. Both ends of the string are functionalized by a bulky stopper (tris(*p*-*tert*-butylphenyl)(4-hydroxyphenyl)methane). Large molecular motions have been induced electrochemically in this molecule and were

detected by using cyclic voltammetry. The driving force of the two rearrangement processes observed is the high stability of two markedly different coordination environments for copper(i) and copper(ii) ions. In the copper(i) state, two phenanthroline units (one of the ring, one of the string) interact with the metal in a tetrahedral geometry ($\text{Cu}^{\text{I}}_{(4)}$), whereas in the copper(ii) state the five-coordinate geometry ($\text{Cu}^{\text{II}}_{(5)}$) is due to the phenanthroline of the string and to

the terpyridine of the ring. The kinetic rate constants of the two molecular motion processes (from $\text{Cu}^{\text{I}}_{(5)}$ to $\text{Cu}^{\text{I}}_{(4)}$ and from $\text{Cu}^{\text{II}}_{(4)}$ to $\text{Cu}^{\text{II}}_{(5)}$) have been determined and both rates are much faster than the ones in previously studied analogous systems. In addition, the rate of the pirouetting motion depends greatly on the copper oxidation state. The divalent four-coordinate copper complex ($\text{Cu}^{\text{II}}_{(4)}$) rearranges in tens of seconds, whereas the monovalent five-coordinate copper system leads to the four-coordinate complex in the millisecond time scale.

Keywords: copper • molecular motions • phenanthroline • rotaxanes • supramolecular chemistry

Introduction

Molecular motors of various kinds are very common in biology.^[1] Roughly, biological motors can be classified in two families: linear and rotary motors. The most classical examples of linear motors are the myosin–actin complex^[2–5] present in muscles or the kinesin-containing system.^[6, 7] Rotary motors have recently attracted much attention since the extremely common enzyme ATP synthase^[8–12] has been shown to behave in a fashion reminiscent of a rotary motor. A „shaft“ (γ protein) rotates inside a hollow stator ($\alpha_3\beta_3$ aggregate of proteins, Figure 1) and this spinning motion induces formation of ATP from ADP and inorganic phosphate (3 moles per round). Another example of a rotary motor is that of bacterial flagella,^[13] which are responsible for bacteria mobility.

The number of synthetic molecular ensembles whose dynamic behavior is reminiscent of biological motors is presently very limited. In order for an object to be regarded

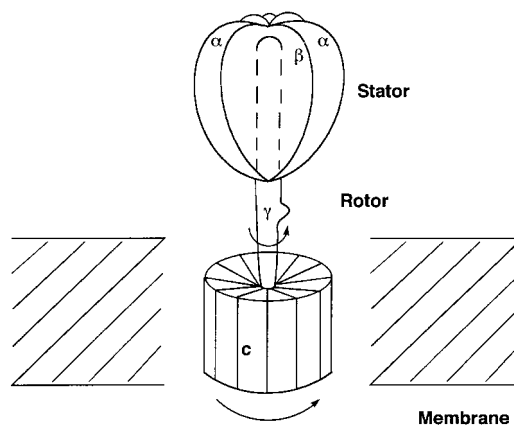


Figure 1. A schematic representation of ATP synthase, a biological rotary motor. γ (and c) are mobile whereas the aggregate $\alpha_3\beta_3$ is fixed to the membrane and constitutes the stator of the motor.

as a motor, several basic requirements have to be fulfilled. Even without trying to apply a strict thermodynamic definition, the system will have to convert a certain type of energy into another form of energy, while undergoing some kind of continuous motion.

Very generally, creating molecules which can change shape, change position in space, or whose certain parts can be set in

[a] Prof. J.-M. Kern, Dr. J.-P. Sauvage, L. Raehm
Institut Le Bel, Université Louis Pasteur
4 rue Blaise Pascal, F-67070 Strasbourg (France)
Fax: (+33)3 88 60 73 12
E-mail: sauvage@chimie.u-strasbg.fr

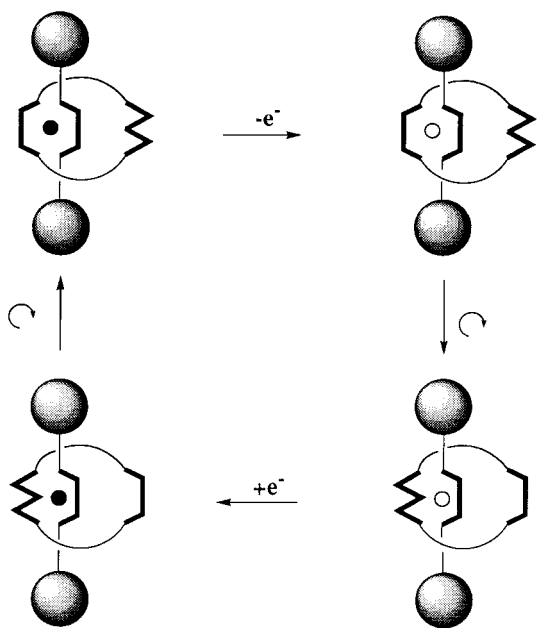


Figure 2. Principle of the electrochemically induced molecular motions in a copper complex rotaxane. The stable four-coordinate monovalent complex is oxidized to an intermediate tetrahedral divalent species. This compound undergoes a rearrangement to afford the stable five-coordinate copper(II) complex. Upon reduction, the five-coordinate monovalent state is formed as transient. Finally, the latter undergoes the reorganization process that regenerates the starting complex (the black circle represents Cu^{I} and the white circle represents Cu^{II}).

motion at will under the action of an external signal, is a challenging target in relation with natural systems mimics but also as components of long-term potential information storage or processing devices.

Results and Discussion

General principle, design, and synthesis

Artificial molecular machines have been described^[14–17]—among them the remarkable work achieved by Stoddart, Balzani, Kaifer and their groups^[18–21]—and special interest was focused on transition metal containing systems.^[22–41] Indeed, the stereoelectronic requirements of a metal center can strongly depend on its oxidation state. Thus, varying the redox state of the metal can lead to a large rearrangement of the surrounding ligands. This is particularly true for copper complexes: Cu^{I} is most of the time low-coordinate (coordination number ≤ 4), whereas Cu^{II} is preferably square planar or higher coordinate (coordination number = 5 or 6). In the systems previously made and investigated in our group,^[42, 43] the same general principle is used: by reducing or oxidizing the copper center, from a sit-

uation corresponding to a stable complex, the system is set out of equilibrium. The relaxation process of the compound implies a large amplitude motion which will bring the system back to its new equilibrium position (Figure 2).

In previous work, gliding motion of a ring around another one (Figure 3 a) in the case of a catenane^[44] or translation motion along a molecular thread (Figure 3 b) in the case of a rotaxane^[43] were studied. Presently, we would like to describe a rotaxane in which a new motion, pirouetting of the wheel around its axle (Figure 3 c), can be electrochemically triggered.

The driving force of this motion is here again based on different geometrical preferences for Cu^{I} and Cu^{II} . The wheel of the rotaxane is a bis-coordinating macrocycle containing both a bidentate moiety, a 1,10-phenanthroline, and a terdentate unit, a 2,2',6',2'',-terpyridine (terpy). The axle incorporates only one bidentate moiety.

The three-dimensional template effect of Cu^{I} , introduced fifteen years ago, made catenanes, rotaxanes, and related systems reasonably accessible from a preparative point of view.^[45–47] The strategy leading to prepare catenanes is based on a precursor consisting of two phenanthroline-type ligands entwined around a Cu^{I} center. In the case where one of these ligands is macrocyclic, the structure of the precursor is particular: the acyclic ligand is threaded through the macrocycle. Reacting the end functions of the acyclic ligand of this complex with an appropriate difunctionalized molecular fragment leads to the formation of a catenane, whereas reacting them with two monofunctionalized and bulky fragments leads to a rotaxane.

An alternative strategy is to use a monostoppered species, to form the prerotaxane intermediate and to add the second stopper afterwards (Figure 4). The advantage of this method,

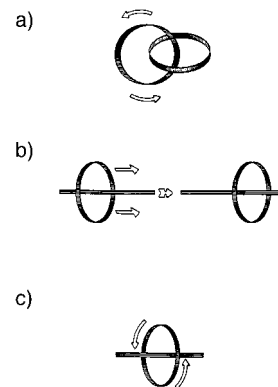


Figure 3. Molecules in motion: a) gliding of a ring around another one; b) translation of a ring along its axle;^[21] c) wheel pirouetting around its axle.

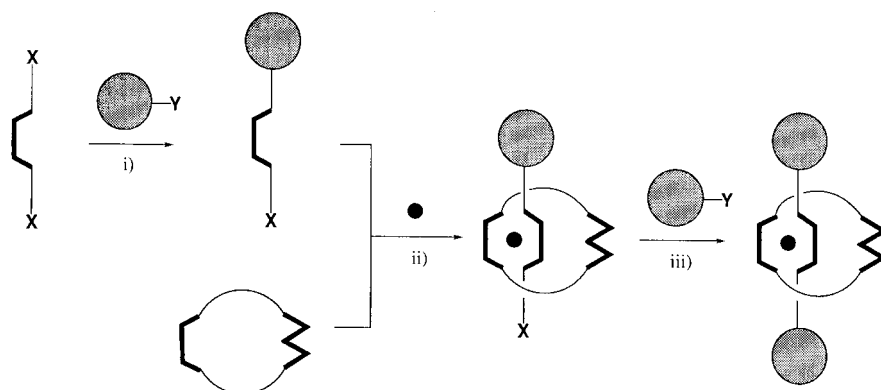


Figure 4. Principle of the synthesis of rotaxane **10**₆₉⁺ (see Figure 5): i) formation of a monostoppered axle; ii) threading of the axle through the wheel; iii) dethreading of the macrocycle is prevented by adding a second blocking group.

which was chosen in the present work, is to limit dethreading of the macrocycle during the stoppering reaction.

The rotaxane $10_{(4)}^+$ (the nomenclature of the rotaxanes described in this work is $10_{(N)}^{n+}$, where N refers to the coordination number of the metal (4 or 5) and n to its charge) synthesized herein is composed of two subunits: a macrocycle and a molecular thread (Figure 5 bottom). The macrocycle^[44] **1** (Figure 5 top) contains two different coordinating sites: a terpyridine moiety and a 1,10-phenanthroline one. A phenanthroline moiety in which the α -positions of the coordinating atoms are substituted with phenyl groups (2,9-diphenyl-1,10-phenanthroline, „dpp“) was used. Indeed, it was shown that the low oxidation state of dpp-based transition metal complexes are strongly stabilized. This is particularly true for copper complexes.^[48] The two units are joined through two C_3 chains which are linked to the 5,5'-positions of the terpyridine on one side and to the 4,4'-positions of the phenanthroline-attached phenyl groups through an oxygen atom each on the other side. The resulting macrocycle **1** has a 33-membered ring.

The molecular thread contains the phenanthroline bidentate unit (dpp). The end groups of the thread, that is the stoppers of the rotaxane, are tetraarylmethane derivatives. These last species were selected as blocking groups since they are large enough to prevent dethreading of the 33-membered ring **1**. In order to lower solubility problems, lipophilic groups (*tert*-butyl fragments) were introduced on the *para* positions of three of the aryl groups. The stoppers and the coordinating site are linked through bisethoxy-ether spacers.

The tetraarylmethane derivative **7** was prepared in four steps starting from compound **3** (tris(*p-tert*-butylphenyl)(4-hydroxyphenyl)methane) whose synthesis has been described by Gibson et al.^[49] Compound **3** was treated with a small excess of THP-protected 2-(2'-iodoethoxy)ethanol (THP = tetrahydropyran-2-yl) to afford **4** in high yield. Transformation of **4** into bromo derivative **7** was done by treatment of the mesylate ester **6** with NaBr in acetone, **6** being prepared by esterification of the alcohol **5**, obtained by hydrolysis of **4**. The monostoppered thread **8** was obtained by reacting the electrophile **7** with a large excess of 2,9-di(*p*-hydroxyphenyl)-1,10-phenanthroline^[50] (**2**) in basic (K_2CO_3) DMF medium. Following this procedure, **8** was isolated in 50% yield, and most of the excess of diphenol **2** could be recovered.

Pre-rotaxane 9^+ was prepared in the following manner: $Cu(CH_3CN)_4BF_4$ ^[51] was added to a solution of **1** in CH_2Cl_2/CH_3CN . The resulting orange-red solution was then treated with **8** to give almost quantitatively a brown-red solution of semi-rotaxane $[9^+]BF_4$. For the preparation of the fully blocked rotaxane $10_{(4)}^+$, 9^+ and **7** were dissolved in DMF, during which the temperature was maintained between 55 and 60 °C, and the base Cs_2CO_3 was added portionwise over 4 h. Indeed, it was observed that dethreading, which occurs in hot and basic medium, is limited using this procedure. The reaction was followed by counterion exchange (KPF_6) to give $[10_{(4)}^+]PF_6$. The overall yield of these two last steps is 30%.

The rotaxane $10_{(4)}^+$ was characterized by FAB-MS, 1H NMR and UV spectroscopy. FAB-MS revealed the threaded structure of the compound; intense peaks corresponding to the loss of the counterion (m/z 2255.2) and to the loss of the counterion and the thread (m/z 740.2) are observed.

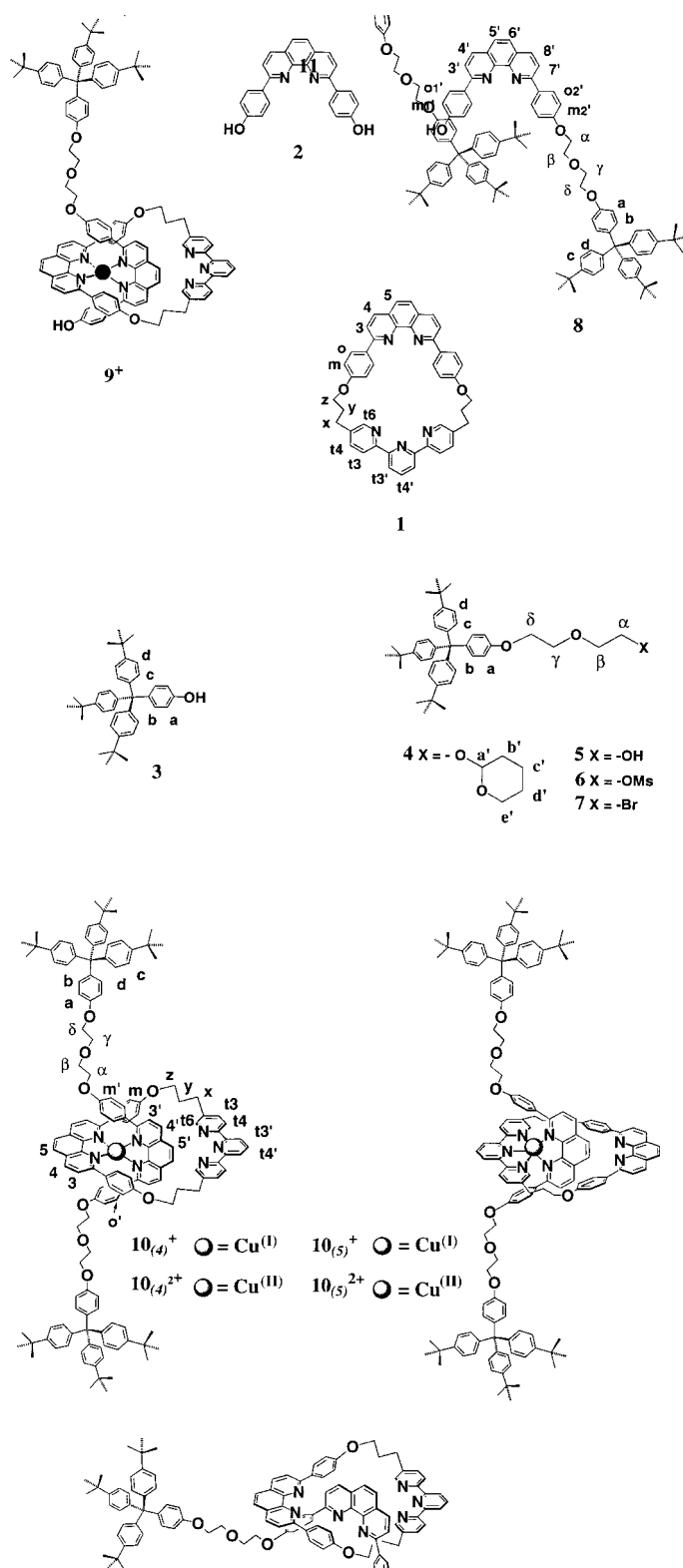


Figure 5. Molecular representation of the metalated rotaxanes $10_{(4)}^+$, $10_{(5)}^+$, $10_{(4)}^{2+}$, $10_{(5)}^{2+}$, of the metal-free rotaxane **11** and of their precursors **1–9**.

^1H NMR spectroscopy (Figure 6a) confirmed the threaded structure of $\mathbf{10}_{(4)}^+$ and the entwining of the two dpp subunits around the metal. Indeed, it shows the usual upfield shifts of the aromatic protons of the phenoxy moieties attached to the phenanthrolines in such intertwined structures.^[52] For instance, a shielding of $\delta = 1.11$ ppm is observed from the *meta* protons of the free ring $\mathbf{1}$ to the corresponding protons (H_m) in

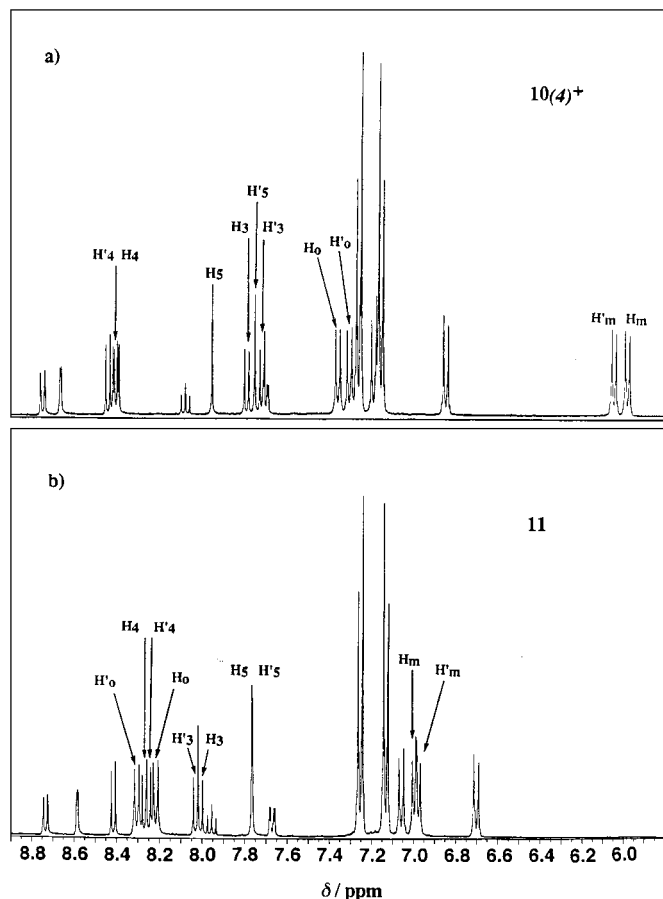


Figure 6. ^1H NMR spectra (field: 400 MHz, solvent: CD_2Cl_2) of a) the Cu^{I} rotaxane $\mathbf{10}_{(4)}^+$ and b) the corresponding metal-free rotaxane $\mathbf{11}$, in the aromatic region. The protons of the two different dpp units undergoing the most significant shift when going from $\mathbf{10}_{(4)}^+$ to $\mathbf{11}$ are labeled; the proton numbering is indicated in Figure 5.

$\mathbf{10}_{(4)}^+$. A similar shift happens for the *meta* protons of the thread: the string precursor $\mathbf{8}$ contains two types of such protons resonating at $\delta = 7.12$ (H'_{m1}) and $\delta = 6.98$ (H'_{m2}), respectively. For $\mathbf{10}_{(4)}^+$, one unique signal at $\delta = 6.02$ corresponds to the four *meta* protons (H'_m) of the string.

As expected, the high MLCT characteristic of the absorption band in the visible range for $\text{Cu}^{\text{I}}(\text{dpp})_2$ -based complexes is observed for $\mathbf{10}_{(4)}^+$ ($\lambda_{\text{max}} = 438$ nm, $\epsilon = 2830$).

The Cu^{I} complex rotaxane $\mathbf{10}_{(4)}^+$ could be easily demetalated^[50] by reaction with cyanide under mild conditions, leading to rotaxane $\mathbf{11}$, with free coordination sites. The FAB-MS of the metal-free $\mathbf{11}$ shows an intense peak at m/z 2192.2 corresponding to the molecular peak ($+\text{H}^+$), and two peaks corresponding to the loss of the ring and to the loss of the thread (m/z 1513.8, m/z 678.3, respectively). In the ^1H NMR spectrum (Figure 6b), a downfield shift of the aromatic

protons (H_o , H'_o , H_m , H'_m) of the phenoxy moieties attached to the phenanthrolines is observed, indicating that the intertwined structure of the two dpp fragments has disappeared. The chemical shift values observed for $\mathbf{11}$ are in the same range as the ones for the free subunits $\mathbf{1}$ and $\mathbf{8}$.

Transformation of the free rotaxane $\mathbf{11}$ into the Cu^{II} complex $\mathbf{10}_{(5)}^{2+}$ was quantitatively achieved by mixing $\mathbf{11}$ with a $\text{CH}_3\text{CN}/\text{CH}_2\text{Cl}_2$ solution of $\text{Cu}^{\text{II}}(\text{BF}_4)_2$. In this case, the structure was confirmed by FAB-MS and the five-coordinate state of the metal was evidenced by UV/Vis spectroscopy: λ_{max} is observed at 618 nm, and this wavelength range is characteristic of Cu^{II} polyimine complexes.^[51] The very low value of the extinction coefficient ($\epsilon = 104$) indicates that the metal is five-coordinate^[42, 44] (which means in the case of $\mathbf{10}_{(5)}^{2+}$ that the copper is surrounded by one dpp and one terpy ligand). For $\text{Cu}^{\text{II}}(\text{dpp})_2$ complexes where the metal can not reasonably be more than tetracoordinate, λ_{max} is around 680 nm and the extinction coefficient is significantly higher^[51] (around 800).

Electrochemical study of the pirouetting motion

The electrochemical behavior of tetracoordinate Cu^{I} complexes that is, $\text{Cu}(\text{dpp})_2$ -based cores, is well established.^[51, 53] The reversible redox potential for the $\text{Cu}^{\text{II}}/\text{Cu}^{\text{I}}$ transition is around 0.6–0.7 V vs. SCE. This relatively high potential underlines the stability of the four-coordinate Cu^{I} complexes versus the corresponding Cu^{II} ones. The redox potential of pentacoordinate copper complexes^[42, 43] is observed in a much more cathodic range. For example, for the five-coordinate complex $\text{Cu}(\mathbf{1}, \text{dap})^{2+/+}$ ($\text{dap} = 2,9$ -di-*p*-anisyl-1,10-phenanthroline), in which the terpy fragment of the ring is bound to the metal, the redox potential is -0.035 V. This potential shift when going from tetracoordinate to pentacoordinate copper systems is due to the better stabilization of the Cu^{II} state thanks to the presence in the coordination sphere of five donor atoms.

a) Electrochemical behaviour of chemically isolated $\mathbf{10}_{(4)}^+$ and $\mathbf{10}_{(5)}^{2+}$: The electrochemical behavior of $\mathbf{10}_{(4)}^+$ in a $\text{CH}_2\text{Cl}_2/\text{CH}_3\text{CN}$ solution has been studied by cyclic voltammetry (CV) and is represented Figure 7a. A reversible signal appears at 0.545 V. The difference of potential ΔE_p between the anodic and the cathodic peak is 70 mV for this signal. A very weak redox peak at -0.15 V can also be observed.

In the rotaxane $\mathbf{10}_{(4)}^+$, where the metal is tetracoordinate, the signal occurring at 0.54 V corresponds to the tetracoordinate $\text{Cu}^{\text{II}}/\text{Cu}^{\text{I}}$ couple. The ratio of the intensities of the anodic and cathodic peaks ipc/ipa is 0.95 (ipc and ipa are the intensity of the cathodic and anodic peaks, respectively), showing that no transformation or reorganization of the coordination sphere of the tetracoordinate Cu^{II} complex occurs in the time scale of the measurements (sweep rate of the potential: 100 mV s^{-1}). We checked that the signal at -0.15 V and the main redox signal are not related. It is probably due to the presence of small amounts of $\mathbf{10}_{(5)}^{2+}$ (vide infra).

The cyclic voltammetry behavior of the Cu^{II} rotaxane $\mathbf{10}_{(5)}^{2+}$ (Figure 7 b), is very different from that of $\mathbf{10}_{(4)}^+$. The potential sweep for the measurement was started at $+0.9$ V, a

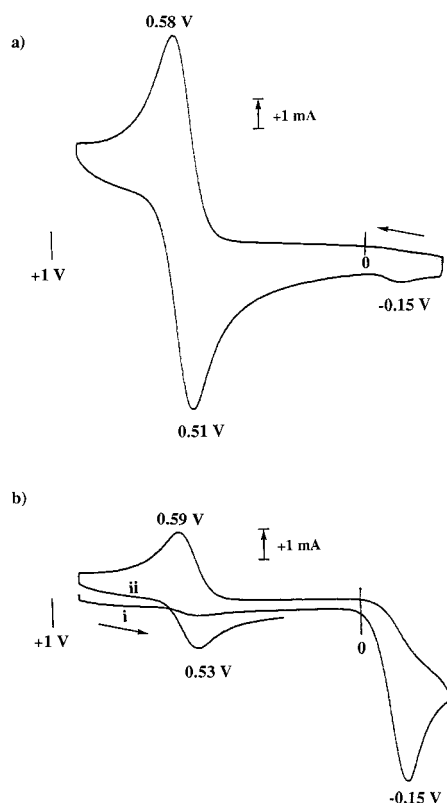


Figure 7. Cyclic voltammograms recorded using a Pt working electrode at a 100 mV s^{-1} sweep rate ($\text{CH}_3\text{CN}/\text{CH}_2\text{Cl}_2$ (4:1), supporting electrolyte: tetrabutylammonium tetrafluoroborate, 0.1 mol L^{-1} , Ag wire pseudo-reference). a) Compound $10_{(4)}^+$, b) chemically prepared $10_{(5)}^{2+}$. Curve ii) refers to a second potential sweep following immediately the first one (i).

potential at which no electron transfer should occur, regardless of the nature of the surrounding of the central Cu^{II} center (penta- or tetracoordinate). Curve i) (first scan, recorded at 100 mV s^{-1}) shows two cathodic peaks: a very small one, located at $+0.53 \text{ V}$ followed by an intense one at -0.15 V . Only one anodic peak at 0.59 V appears during the reverse sweep. If a second scan ii) follows immediately the first one i), the intensity of the cathodic peak at 0.53 V increases noticeably.

The weak peak at 0.53 V (i, Figure 7b) is due to the presence of small quantities of $10_{(4)}^+$. The main cathodic peak at -0.15 V is characteristic of pentacoordinate Cu^{II} . Thus, in $10_{(5)}^{2+}$ prepared from the free rotaxane by metalation with Cu^{II} ions, the central metal is coordinated to the terdentate terpyridine of the wheel and to the bidentate dpp of the axle. On the other hand, the irreversibility of this peak means that the pentacoordinate Cu^{I} species formed in the diffusion layer when sweeping cathodically is transformed very rapidly and in any case before the electrode potential becomes again more anodic than the potential of the pentacoordinate $\text{Cu}^{2+}/\text{Cu}^+$ redox system. The irreversible character of the wave at -0.15 V and the appearance of an anodic peak at the value of $+0.53 \text{ V}$ indicates that the transient species, formed by reduction of $10_{(5)}^{2+}$, has undergone a complete reorganization, which leads to a tetracoordinate copper rotaxane. The second scan (ii) which follows immediately the first one (i) confirms this assertion. Indeed, a cathodic peak ($+0.53 \text{ V}$) has ap-

peared, corresponding to the reduction of this tetracoordinate species.

These two complementary cyclic voltammetry experiments confirm that in this rotaxane, like in previously studied related systems, the tetracoordinate Cu^{I} state is more stable than the pentacoordinate one and the pentacoordinate Cu^{II} state is more stable than the tetracoordinate one. Moreover, it was observed that the rearrangement rates from the less to the most stable geometries are drastically different for the two oxidation states of the metal.

The irreversibility of the reduction peak of $10_{(5)}^{2+}$, combined with the appearance of a reversible peak corresponding to tetracoordinate copper, suggests that the reorganization of the rotaxane in its pentacoordinate form $10_{(5)}^+$ (that is, with the copper being coordinated to terpy and to dpp units), to its tetracoordinate form ($10_{(4)}^+$, where the copper is surrounded by two dpp units) occurs within the time scale of the cyclic voltammetry. CV measurements at high potential sweep rates is therefore a well-suited method to study the reorganization kinetics of such systems. On the other hand, Figure 7a indicates the inertness of the reorganization of the tetracoordinate Cu^{II} rotaxane, and cyclic voltammetry is thus inappropriate to study the kinetic of such a system. Therefore, a total conversion of tetracoordinate $10_{(4)}^+$ to tetracoordinate $10_{(4)}^{2+}$ was performed by preparative electrolysis and the subsequent rearrangement of tetracoordinate $10_{(4)}^{2+}$ into pentacoordinate $10_{(5)}^{2+}$ was monitored by an amperometric method.

b) Determination of the kinetic rate constant k for the transformation of pentacoordinate Cu^{I} into tetracoordinate Cu^{I} : $10_{(5)}^+ \rightarrow 10_{(4)}^+$: Figure 8 illustrates the evolution of the cyclic voltammetry response of pentacoordinate $10_{(5)}^{2+}$ when scanning the potential at different sweep rates, going from $\nu = 500 \text{ mV s}^{-1}$ to $\nu = 8 \text{ V s}^{-1}$. It was observed that the system became progressively reversible.

The behavior of the I/E (current/potential) curves at different sweep rates is typical for the case where an electron transfer is followed by an irreversible chemical reaction (transformation of pentacoordinate $10_{(5)}^+$ into tetracoordinate $10_{(4)}^+$). This qualitative observation was confirmed by the numeric exploitation of the I/E responses, following the method described by Nicholson and Shain.^[54] For each curve, the $i_{\text{pa}}/i_{\text{pc}}$ ratio was measured as well as $E_{1/2}$ (half-wave potential). Thus, parameter τ could be calculated from Equation (1), where ν = sweep rate and E_{λ} = inversion potential.

$$\tau = (E_{\lambda} - E_{1/2})/\nu \quad (1)$$

Using the working curve established by the authors, the value of $\log(k\tau)$ could be determined and thus, k extracted. In order to obtain an accurate k value, several curves were studied, varying both ν and the inversion potential. An average value of $17 \pm 9 \text{ s}^{-1}$ was found for k . In other words, in this medium (acetonitrile/dichloromethane (4/1), Bu_4NBF_4 ($10^{-1} \text{ mol L}^{-1}$), room temperature), the half-life time of pentacoordinate Cu^{I} rotaxane is $56 \pm 28 \text{ ms}$ ($t_{1/2} = \ln 2/k$).

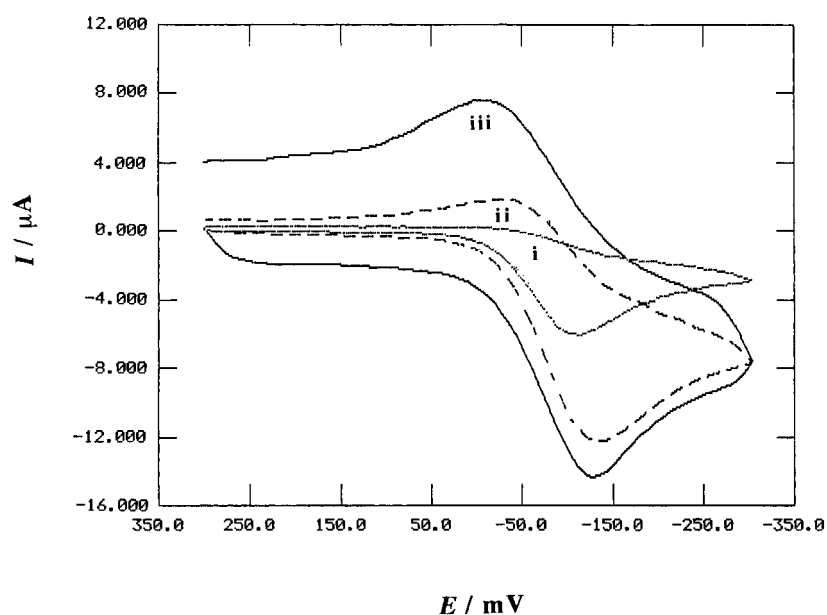


Figure 8. Illustration of the evolution of the CV curves of $\mathbf{10}_{(5)}^{2+}$ when increasing the potential sweep rate (same conditions as indicated in Figure 7). i) $v = 500 \text{ mV s}^{-1}$, ii) $v = 3000 \text{ mV s}^{-1}$, iii) $v = 8000 \text{ mV s}^{-1}$.

c) Determination of the kinetic rate constant k' for the transformation of tetracoordinate Cu^{II} into pentacoordinate Cu^{II} : $\mathbf{10}_{(4)}^{2+} \rightarrow \mathbf{10}_{(5)}^{2+}$: As illustrated by the cyclic voltammetry curve represented in Figure 7a and discussed above, the tetracoordinate Cu^{II} rotaxane generated in the diffusion layer does not undergo any detectable rearrangement during the reverse potential scanning. Indeed, at small sweep rates (100 mV s^{-1} or 50 mV s^{-1}), the ratio $i_{\text{pa}}/i_{\text{pc}}$ remains near to one and no increase of the cathodic peak at -0.15 V occurs. The $E_{1/2}$ values of $\mathbf{10}_{(4)}^{2+}/\mathbf{10}_{(4)}^{+}$ and $\mathbf{10}_{(5)}^{2+}/\mathbf{10}_{(5)}^{+}$ are $+0.55 \text{ V}$ and -0.1 V , respectively. Thus, when polarizing the working electrode at a potential between these two values, under stationary conditions (by using a rotating disk electrode, for example), the cathodic current observed is representative of the presence and concentration of $\mathbf{10}_{(4)}^{2+}$, the tetracoordinate Cu^{II} complex only. This remains true even if the electrolytic solution contains pentacoordinate $\mathbf{10}_{(5)}^{2+}$ which will be electrochemically silent in the potential range used.

A solution of $\mathbf{10}_{(4)}^{+}$ was anodically electrolyzed into the Cu^{II} state as quickly as possible, using an electrolytic cell with an high S/V value (S = electrode surface, V = volume of the electrolytic solution). A rotating disk electrode was then introduced in the solution and polarized at $+0.3 \text{ V}$. Current versus time was recorded and an exponential decrease of the intensity of the current was observed. When the current was near to 0, a new cyclic voltammetry curve of the solution was measured, leading to a voltammogram similar to the one represented Figure 7b. This confirms that the electrogenerated tetracoordinate Cu^{II} rotaxane has undergone a rearrangement to form the pentacoordinate Cu^{II} rotaxane $\mathbf{10}_{(5)}^{2+}$.

The kinetic constant of this transformation can be extracted from the variation of the cathodic current. Indeed, the logarithm of this current intensity vs. time is linear (Figure 9), as expected for a monomolecular process. The value of k' is given by the slope of this straight line. The average value of k' in this rearrangement is $0.007 \pm 0.003 \text{ s}^{-1}$. In other words, the

half-life time of tetracoordinate Cu^{II} rotaxane is $120 \pm 50 \text{ s}$.

d) Conclusion: These experiments underline the noticeable difference of the kinetic rate constants k and k' for the reorganization processes leading from $\mathbf{10}_{(5)}^{+}$ to $\mathbf{10}_{(4)}^{+}$ and from $\mathbf{10}_{(4)}^{2+}$ to $\mathbf{10}_{(5)}^{2+}$, respectively. Indeed, the ratio k/k' is about 3000:1. In the analogous systems already studied,^[42, 43] an important difference between the related rate constants had also been observed. Nevertheless, for the systems based on a copper [2]cate-nate,^[42, 44] where one of the macrocycles is monochelating and the other one hetero-bis-

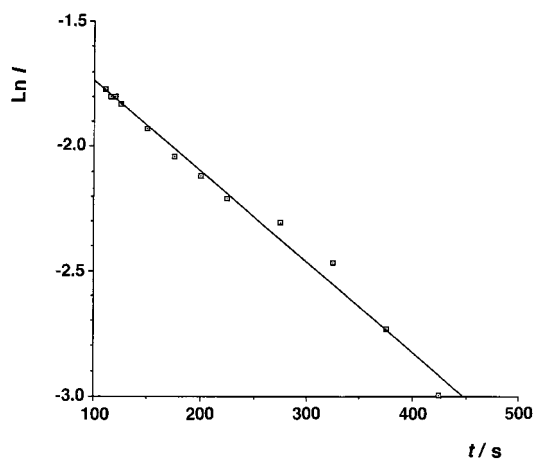


Figure 9. Representation of the logarithmic decay of the current intensity versus time of a solution of $\mathbf{10}_{(4)}^{2+}$ obtained by anodic electrolysis of $\mathbf{10}_{(4)}^{+}$. The working electrode is a rotating Pt disk electrode ($\omega = 6300 \text{ rad s}^{-1}$), polarized at $+0.3 \text{ V}$ vs. Ag wire pseudo-reference.

chelating, the two processes are much slower. In addition, reproducibility problems made the accurate measurement of the corresponding rate constants difficult, especially for the rearrangement from $\text{Cu}_{(4)}^{\text{II}}$ to $\text{Cu}_{(5)}^{\text{II}}$. The reorganization around Cu^{I} takes about 1 s and the one around Cu^{II} takes as much as several days, depending on the medium. For the rotaxane^[43] where the axle is a hetero-bischelating molecular thread and the wheel a monochelating macrocycle, the reorganization processes which imply a translation of the ring along the string, the values determined for k and k' are 10^{-2} and $1.5 \times 10^{-4} \text{ s}^{-1}$, respectively. Thus, by comparison with the rate constant values determined for the rotaxane studied in this work ($k = 17$ and $k' = 0.007 \text{ s}^{-1}$), it appears that pirouetting of a macrocycle around its axle induced by changing the redox state of the central metal is also faster than the translation of a macrocycle along a molecular thread, using the same triggering process.

These different types of molecular motion: gliding, translating and pirouetting are possible thanks to the kinetic lability of copper complexes. As mentioned above, the k/k' ratio is high in all the cases studied so far, which means that the reorganization process around Cu^I is much faster than around Cu^{II} . Both rearrangements require a decoordination step of one of the chelates, followed by recomplexation by the other chelate. The activation barrier of this decoordination step might be higher for the tetracoordinate Cu^{II} to pentacoordinate Cu^{II} process than for the pentacoordinate Cu^I to tetracoordinate Cu^I one, due to the higher electronic requirements of Cu^{II} . Thus, the difference of molecular motion rates induced by changing the redox state of the metal could be partially attributed to the ligand field effect.

Conclusion

The presently described system represents a first step towards the elaboration of rotary motors at the molecular level. At the present stage, the bifunctional ring can only oscillate between two positions on the axle on which it is threaded. This process is now well controlled and reasonably fast, especially for the monovalent copper(I) complex rearrangement. In order to make real rotary motors, it will be necessary to introduce directionality in the system by using, among other possibilities, a ring containing three different coordination sites and a directed axle. The synthesis of such multicomponent compounds is presently under way.

Experimental Section

Synthesis of 4: Compound **3** (1 g, 1.98 mmol) and 2-(2-iodoethoxy)ethyl 2-tetrahydro-2H-pyran ether (740 mg, 2.46 mmol) were dissolved in DMF (50 mL) in a 100-mL round-bottomed flask equipped with a condenser. Potassium carbonate (1.4 g, 10 mmol) was added and the solution was degassed before being heated at 60 °C under argon for 17 h. DMF was removed and the residue was taken up into $\text{H}_2\text{O}/\text{CH}_2\text{Cl}_2$. Extraction with CH_2Cl_2 and drying over Na_2SO_4 left, after the solvent was removed, a white powder whose purity was sufficient (>95% by NMR) to be used without further purification. White powder; ^1H NMR (200 MHz, CDCl_3): δ = 7.25 (d, J = 8.6 Hz, 8H; $\text{H}_{\text{b,c}}$), 7.07 (d, J = 8.6 Hz, 6H; H_d), 6.78 (d, J = 8.8 Hz, 2H; H_a), 4.65 (t, 1H; H_e), 4.12 (m, 2H; H_f), 3.8–3.4 (m, 12H; $\text{H}_{\alpha,\beta,\gamma} + \text{H}_{\text{b',c',d',e'}}$), 1.31 (s, 27H; CH_3).

Synthesis of 5: Compound **4** (1.32 g, 1.96 mmol) was dissolved in CHCl_3 (15 mL) in a 100-mL round-bottomed flask equipped with a condenser. EtOH (20 mL) was added and the solution was heated at 80 °C. HCl 36% (1 mL, catalytic) was then added and the mixture was refluxed for 18 h. The solvents were removed and the residue was taken up into $\text{H}_2\text{O}/\text{CH}_2\text{Cl}_2$. The opaque organic layer was washed with a saturated solution of K_2CO_3 in H_2O and then with pure H_2O to give a translucent organic layer. Drying over Na_2SO_4 left, after the solvent was removed, a white powder which was purified by flash column chromatography (SiO_2 , eluent CH_2Cl_2) to afford **5** in 82% yield (944 mg, 1.61 mmol). White powder; ^1H NMR (200 MHz, CDCl_3): δ = 7.24 (d, J = 8.6 Hz, 8H; $\text{H}_{\text{b,c}}$), 7.08 (d, J = 8.6 Hz, 6H; H_d), 6.79 (d, J = 8.8 Hz, 2H; H_a), 4.12 (m, 2H; H_f), 3.87 (m, 2H; H_g), 3.8–3.6 (m, 4H; $\text{H}_{\beta,\gamma}$), 1.32 (s, 27H; CH_3).

Synthesis of 6: Methyl chloride (0.62 mL, 7.97 mmol) dissolved in CH_2Cl_2 (8 mL) was added over 40 min to a solution of **5** (944 mg, 1.59 mmol) in CH_2Cl_2 (30 mL) at -5°C containing triethylamine (2.8 mL, 2.03 g, 20 mmol). After stirring for 3 h at -5°C , the solution was extracted with $\text{H}_2\text{O}/\text{CH}_2\text{Cl}_2$ and dried over Na_2SO_4 . The solvents were removed and the crude product was filtered by flash chromatography (SiO_2 , eluent CH_2Cl_2) to afford **6** (900 mg, 1.33 mmol) in 84% yield. White powder; m.p. 231 °C;

^1H NMR (200 MHz, CDCl_3): δ = 7.24 (d, J = 8.6 Hz, 8H; $\text{H}_{\text{b,c}}$), 7.07 (d, J = 8.6 Hz, 6H; H_d), 6.78 (d, J = 8.8 Hz, 2H; H_a), 4.40 (m, 2H; H_f), 4.10 (m, 2H; H_g), 3.9–3.8 (m, 4H; $\text{H}_{\beta,\gamma}$), 3.04 (s, 3H; CH_3), 1.32 (s, 27H; CH_3); MS (MALDI-TOF MS): m/z : 670.64 ($[\text{M} + \text{H}]^+$, 670.95).

Synthesis of 7: After being degassed, a solution of **6** (900 mg, 1.34 mmol) and LiBr (780 mg, 8.96 mmol) in acetone (30 mL) was refluxed for 3 h under argon (70 °C). Acetone was removed and the residue was taken up into $\text{H}_2\text{O}/\text{CH}_2\text{Cl}_2$. Extraction with CH_2Cl_2 and drying over Na_2SO_4 left, after the solvent was removed, a white powder (857 mg) whose purity was sufficient (>95% by NMR spectroscopy) to be used without further purification. White powder; m.p. 183 °C; ^1H NMR (200 MHz, CDCl_3): δ = 7.24 (d, J = 8.6 Hz, 8H; $\text{H}_{\text{b,c}}$), 7.09 (d, J = 8.6 Hz, 6H; H_d), 6.77 (d, J = 8.8 Hz, 2H; H_a), 4.12 (m, 2H; H_f), 4–3.8 (m, 4H; $\text{H}_{\beta,\gamma}$), 3.46 (m, 2H; H_g), 1.31 (s, 27H; CH_3); elemental analysis calcd (%) for $\text{C}_{41}\text{H}_{51}\text{O}_2\text{Br}$: C 75.10, H 7.84; found C 75.39, H 8.09.

Synthesis of 8: Compound **7** (100 mg, 1.49 mmol) and 2,9-di(*p*-hydroxyphenyl)-1,10-phenanthroline (271 mg, 0.75 mmol) were dissolved in DMF (50 mL) in a 100-mL round-bottomed flask equipped with a condenser. The solution was then degassed and K_2CO_3 (513 mg, 3.7 mmol) was added. The mixture was heated at 60 °C for 18 h under argon. DMF was removed and the residue was taken up in $\text{H}_2\text{O}/\text{CH}_2\text{Cl}_2$. Extraction with CH_2Cl_2 and drying over Na_2SO_4 left, after the solvent was removed, a bright orange powder which was purified by flash chromatography (SiO_2 , eluent $\text{CH}_2\text{Cl}_2/\text{MeOH}$ 1%) to afford **8** (70 mg, 0.73 mmol) in 49% yield. Bright orange solid; ^1H NMR (200 MHz, CDCl_3): δ = 8.40 (d, J = 8.8 Hz, 2H; $\text{H}_{\text{O}1}$), 8.29 (d, J = 8.8 Hz, 2H; $\text{H}_{\text{O}2}$), 8.26 (d, J = 8.4 Hz, 1H; H_7), 8.25 (d, J = 8.6 Hz, 1H; H_4), 8.06 (d, J = 8.6 Hz, 1H; H_8), 8.04 (d, J = 8.4 Hz, 1H; H_3), 7.75 (s, 2H; $\text{H}_{5,6}$), 7.26 (d, J = 8.6 Hz, 8H; $\text{H}_{\text{b,c}}$), 7.12 (d, J = 8.6 Hz, 2H; $\text{H}_{\text{m}1}$), 7.12 (d, J = 8.4 Hz, 6H; H_d), 6.98 (d, J = 8.6 Hz, 2H; $\text{H}_{\text{m}2}$), 6.82 (d, J = 8.8 Hz, 2H; H_a), 4.27 (m, J = 4.3 Hz, 2H; H_e), 4.17 (m, J = 4.3 Hz, 2H; H_f), 4–3.9 (m, 4H; $\text{H}_{\beta,\gamma}$), 1.32 (s, 27H; CH_3); MS (MALDI-TOF MS): m/z : 940.14 ($[\text{M} + \text{H}]^+$, 939.25).

Synthesis of 9⁺: A solution of $\text{Cu}(\text{CH}_3\text{CN})_4\text{BF}_4$ (57.3 mg, 0.182 mmol) in degassed acetonitrile (5 mL) was added by canula to a stirred degassed solution of **1** (123.5 mg, 0.182 mmol) in degassed CH_2Cl_2 (10 mL) at room temperature. A brown-orange coloration appeared instantaneously. After stirring for 30 min at room temperature, a solution of **8** (158 mg, 0.166 mmol) in degassed CH_2Cl_2 (10 mL) was added to the previous mixture by the canula transfer technique and the solution immediately turned dark red. The solution was stirred for one hour under argon. After the solvents were removed, a dark red solid of crude **9⁺** was obtained in a nearly quantitative yield (285 mg). The purity of **9⁺** was sufficient (>95% by NMR spectroscopy) to be used without further purification. Dark red solid; ^1H NMR (400 MHz, CD_2Cl_2): δ = 8.64 (d, J = 8.4 Hz, 2H; t_3), 8.57 (d, 2H; t_6), 8.43 (d, J = 8.6 Hz, 2H; t_5), 8.37 (d, J = 8 Hz, 2H; $\text{H}_{4,7}$), 8.29 (d, J = 7.8 Hz, 2H; $\text{H}_{4,7}$), 8.06 (t, J = 7.6 Hz, 1H; t_4), 7.92 (s, 2H; $\text{H}_{5,6}$), 7.72 (s, 2H; $\text{H}_{5,6}$), 7.9–7.6 (m, 6H; $\text{H}_{3,8}$, $\text{H}_{3,8}$, t_4), 7.36 (d, J = 8.5 Hz, 4H; H_d), 7.31 (d, J = 8.5 Hz, 4H; $\text{H}_{\text{O}1,\text{O}2}$), 7.18 (d, J = 8.6 Hz, 8H; $\text{H}_{\text{b,c}}$), 7.07 (d, J = 8.6 Hz, 6H; H_d), 6.80 (d, J = 8.8 Hz, 2H; H_a), 6–5.9 (m, 8H; H_m , $\text{H}_{\text{m}1}$, $\text{H}_{\text{m}2}$), 4.04 (m, 2H; H_e), 3.84 (m, 2H; H_f), 3.65 (m, 4H; $\text{H}_{\beta,\gamma}$), 3.25 (m, 4H; H_g), 2.90 (m, 4H; H_z), 2.10 (m, 4H; H_y), 1.32 (s, 27H; CH_3).

Synthesis of 10⁺: Complex **9⁺** (285 mg, 0.16 mmol) and **7** (128.5 mg, 0.19 mmol) were dissolved in DMF (16 mL) in a 100-mL Schlenk flask. The solution was degassed and heated at 58 °C. Cs_2CO_3 (520 mg, 1.6 mmol), maintained in suspension in DMF (5 mL) in an addition funnel thanks to bubbling argon, was added dropwise over 4 h under argon. The solution was then stirred under argon for an additional 15 h. DMF was removed and the residue was taken up in $\text{H}_2\text{O}/\text{CH}_2\text{Cl}_2$ and dried over Na_2SO_4 . Before purification, the counterions were exchanged from BF_4 to PF_6 , following a well-known procedure. The product was then purified by column chromatography (SiO_2 , eluent $\text{CH}_2\text{Cl}_2/\text{MeOH}$ 2%) to afford **10⁺** (120 mg, 0.048 mmol) in 30% yield. Dark red solid. ^1H ROESY NMR (400 MHz, CD_2Cl_2): δ = 8.75 (d, J = 8.1 Hz, 2H; t_3), 8.62 (d, 2H; t_6), 8.40 (d, J = 7.9 Hz, 2H; t'_3), 8.39 (d, J = 8.4 Hz, 2H; $\text{H}_{4,7}$), 8.37 (d, J = 8.4 Hz, 2H; H_d), 8.04 (t, J = 7.8 Hz, 1H; t_4), 7.93 (s, 2H; $\text{H}_{5,6}$), 7.75 (d, J = 8.4 Hz, 2H; H_3), 7.71 (s, 2H; $\text{H}_{5,6}$), 7.68 (d, J = 8.4 Hz, 2H; $\text{H}_{3,8}$), 7.66 (dd, J = 8.1 Hz, 2H; t_4), 7.32 (d, J = 8.8 Hz, 4H; H_e), 7.27 (d, J = 8.8 Hz, 4H; H_f), 7.21 (d, J = 8.6 Hz, 12H; H_g), 7.15 (d, J = 8.8 Hz, 4H; H_h), 7.11 (d, J = 8.6 Hz, 12H; H_d), 6.81 (d, J = 9 Hz, 4H; H_a), 6.01 (d, J = 8.8 Hz, 4H; H_m), 5.94 (d, J = 8.9 Hz, 4H; H_m), 4.13 (m, 4H; H_e), 3.84 (m, 4H; H_f), 3.74 (m, 4H; H_g), 3.67 (m, 4H;

H₁), 3.19 (m, 4H; H_z), 2.90 (m, 4H; H_x), 2.10 (m, 4H; H_y), 1.26 (s, 54H; CH₃); MS (FAB-MS): *m/z*: 2255.2 ([M – PF₆]⁺, 2255.5).

Synthesis of 11: Complex 10⁺ (40 mg, 16.6 μmol) was dissolved in CH₂Cl₂ (5 mL). KCN (26 mg; 0.38 mmol) was dissolved in water (1 mL) and added to the former solution. CH₃CN (2 mL) was added to the mixture and the solution was stirred for 30 min before more CH₃CN (2 mL) was added. The solution was stirred until the initially dark red color had totally disappeared (about 1 h). The mixture was then extracted with CH₂Cl₂ and the resulting organic layer was carefully washed with water and dried over Na₂SO₄. The water was discarded by pouring it into a solution of sodium hypochlorite. CH₂Cl₂ was removed to afford the demethylated rotaxane 11 as a colorless solid (36 mg) quantitatively. Colorless solid; δ = 8.68 (d, *J* = 8.1 Hz, 2H; t₃), 8.53 (d, 2H, *J* = 1.8 Hz; t₆), 8.36 (d, *J* = 7.9 Hz, 2H; t₃), 8.25 (d, *J* = 8.9 Hz, 4H; H_o), 8.21 (d, *J* = 8.6 Hz, 2H; H_d), 8.19 (d, *J* = 8.4 Hz, 2H; H_{4,7}), 8.16 (d, *J* = 8.9 Hz, 4H; H_o), 7.98 (d, *J* = 8.6 Hz, 2H; H_{3,8}), 7.96 (d, *J* = 8.6 Hz, 2H; H₃), 7.90 (t, *J* = 8, 2.2 Hz, 1H; t₄), 7.71 (s, 4H; H_{5,6}, H_{5,6}), 7.61 (dd, *J* = 8 Hz, 2H; t₁), 7.20 (d, *J* = 8.6 Hz, 12H; H_c), 7.07 (d, *J* = 8.6 Hz, 12H; H_d), 7.00 (dd, *J* = 8.6 Hz, 4H; H_b), 6.94 (d, *J* = 8.8 Hz, 4H; H_m), 6.92 (d, *J* = 8.8 Hz, 4H; H_m), 6.65 (d, *J* = 8.8 Hz, 4H; H_a), 4.06 (m, 4H; H_o), 4.00 (m, 4H; H_o), 3.79 (m, 12H; H_z, H_z), 2.86 (m, 4H; H_x), 2.08 (m, 4H; H_y), 1.28 (s, 54H; CH₃); MS (FAB-MS): *m/z*: 2192.2 ([M + H]⁺, 2191.9).

Synthesis of 10_(S)²⁺: Complex 11 (15.56 mg, 7 μmol) was introduced in a 10-mL flask and 1 mL of a 7 mm pale blue solution of Cu^{II}(BF₄)₂ in CH₃CN (i.e. 7 μmol) was added. The solution turned pale green and the volume was brought up to 10 mL with CH₃CN. This solution was used for both UV and CV experiments. Part of it was evaporated to give the mass characterization. Pale green solid; MS (FAB-MS): *m/z*: 2255.1 ([M – PF₆]⁺, 2255.5).

Electrochemistry: Electrochemical experiments were carried out using an EGG Princeton 273 A model potentiostat. All experiments were run at room temperature. For analytical experiments, a standard three-electrode cell was used. Potentials are referenced to an Ag wire pseudo-reference electrode with 0.1 mol L⁻¹ tetrabutylammonium tetrafluoroborate as supporting electrolyte in an acetonitrile/dichloromethane (4/1) mixture as solvent. A platinum disc electrode (2 mm diameter) was used for CV experiments. A platinum wire (0.6 mm diameter, 52 cm long) was used as working electrode for electrolysis at controlled potential.

Acknowledgment

We are grateful to the French Ministry of Education for a fellowship to L.R.

- [1] J. Howard, *Nature* **1997**, *389*, 561–567.
- [2] K. Kitamura, M. Tokunaga, A. H. Iwane, T. Yanagida, *Nature* **1999**, *397*, 129–134.
- [3] I. Rayment, H. M. Holden, M. Whittaker, C. B. Yohn, M. Lorenz, K. C. Holmes, R. A. Milligan, *Science* **1993**, *261*, 58–64.
- [4] I. Rayment, W. R. Rypniewski, K. Schmidt-Bäse, R. Smith, D. R. Tomchick, M. M. Benning, D. A. Winkelmann, G. Wesenberg, H. M. Holden, *Science* **1993**, *261*, 50–58.
- [5] I. Dobbie, M. Linari, G. Piazzesi, M. Reconditi, N. Koubassova, M. A. Ferenczi, V. Lombardi, M. Irving, *Nature* **1998**, *396*, 383–387.
- [6] E. P. Sablin, F. J. Kull, R. Cooke, R. D. Vale, R. J. Fletterick, *Nature* **1996**, *380*, 555–559.
- [7] F. J. Kull, E. P. Sablin, R. Lau, R. J. Fletterick, R. D. Vale, *Nature* **1996**, *380*, 550–555.
- [8] J. P. Abrahams, A. G. W. Leslie, R. Lutter, J. E. Walker, *Nature* **1994**, *370*, 621–628.
- [9] H. Noji, R. Yasuda, M. Yoshida, K. Kinosita, *Nature* **1997**, *386*, 299–302.
- [10] J. E. Walker, *Angew. Chem.* **1998**, *110*, 2438–2450; *Angew. Chem. Int. Ed.* **1998**, *37*, 2308–2319.
- [11] W. S. Allison, *Acc. Chem. Res.* **1998**, *31*, 819–826.
- [12] P. D. Boyer, *Angew. Chem.* **1998**, *110*, 2424–2436; *Angew. Chem. Int. Ed.* **1998**, *37*, 2296–2307.
- [13] L. Stryer in *Biochemistry*, 2nd ed., W. H. Freeman, San Francisco, **1981**, pp. 906–907.
- [14] H. L. Schenck, G. P. Dado, S. H. Gellman, *J. Am. Chem. Soc.* **1996**, *118*, 12487–12494.
- [15] F. Würthner, J. Rebek, Jr., *Angew. Chem.* **1995**, *107*, 503–505; *Angew. Chem. Int. Ed. Engl.* **1995**, *34*, 446–448.
- [16] T. R. Kelly, J. P. Stestelo, I. Tellitu, *J. Org. Chem.* **1998**, *63*, 3655–3665.
- [17] A. C. Benniston, *Chem. Soc. Rev.* **1996**, 428–435.
- [18] V. Balzani, M. Gómez-López, J. F. Stoddart, *Acc. Chem. Res.* **1998**, *31*, 405–414.
- [19] P. R. Ashton, R. Ballardini, V. Balzani, I. Baxter, A. Credi, M. C. T. Fyfe, M. T. Gandolfi, M. Gómez-López, M.-T. Martínez-Díaz, A. Piersanti, N. Spencer, J. F. Stoddart, M. Venturi, A. J. P. White, D. J. Williams, *J. Am. Chem. Soc.* **1998**, *120*, 11932–11942.
- [20] M. Asakawa, S. Iqbal, J. F. Stoddart, N. D. Tinker, *Angew. Chem.* **1996**, *108*, 1054–1056; *Angew. Chem. Int. Ed. Engl.* **1996**, *35*, 976–978.
- [21] R. A. Bissel, E. Córdova, A. E. Kaifer, J. F. Stoddart, *Nature* **1994**, *369*, 133–137.
- [22] G. D. Santis, L. Fabbri, D. Iacopino, P. Pallavicini, A. Perotti, A. Poggi, *Inorg. Chem.* **1997**, *36*, 827–832.
- [23] P. Wittung-Stafshede, B. G. Malmström, J. R. Winkler, H. B. Gray, *J. Phys. Chem.* **1998**, *102*, 5299–5601.
- [24] A. Ikeda, T. Tsudera, S. Shinkai, *J. Org. Chem.* **1997**, *62*, 3568–3574.
- [25] S. Zahn, J. W. Canary, *Angew. Chem.* **1998**, *110*, 321–323; *Angew. Chem. Int. Ed.* **1998**, *37*, 305–307.
- [26] J. Vacek, J. Michl, *New J. Chem.* **1997**, *21*, 1259–1268.
- [27] P. R. Ashton, V. Balzani, O. Kocian, L. Prodi, N. Spencer, J. F. Stoddart, *J. Am. Chem. Soc.* **1998**, *120*, 11190–11191.
- [28] C. Canevet, J. Libman, A. Shanzer, *Angew. Chem.* **1996**, *108*, 2842–2845; *Angew. Chem. Int. Ed. Engl.* **1996**, *35*, 2657–2660.
- [29] M. M. Bernardo, P. V. Robandt, R. R. Schroeder, D. B. Rorabacher, *J. Am. Chem. Soc.* **1989**, *111*, 1224–1231.
- [30] T. T. Chin, W. E. Geiger, A. L. Rheingold, *J. Am. Chem. Soc.* **1996**, *118*, 5002–5010.
- [31] N. E. Katz, F. Fagalde, *Inorg. Chem.* **1993**, *32*, 5391–5393.
- [32] J. Moraczewski, C. A. Sassano, C. A. Mirkin, *J. Am. Chem. Soc.* **1995**, *117*, 11379–11380.
- [33] M. Sano, H. Taube, *J. Am. Chem. Soc.* **1991**, *113*, 2327–2328.
- [34] M. Sano, H. Taube, *Inorg. Chem.* **1994**, *33*, 705–709.
- [35] M. Sano, H. Sago, A. Tomita, *Bull. Chem. Soc. Jpn.* **1996**, *69*, 977–981.
- [36] A. Tomita, M. Sano, *Inorg. Chem.* **1994**, *33*, 5825–5830.
- [37] A. Tomita, M. Sano, *Chem. Lett.* **1996**, 981–982.
- [38] J. W. E. Geiger, *J. Am. Chem. Soc.* **1979**, *101*, 3407–3408.
- [39] J. A. Wytko, C. Boudon, J. Weiss, M. Gross, *Inorg. Chem.* **1996**, *35*, 4469–4470.
- [40] L. Zelikovich, J. Libman, A. Shanzer, *Nature* **1995**, 790–792.
- [41] E. T. Singewald, C. A. Mirkin, C. L. Stern, *Angew. Chem.* **1995**, *107*, 1725–1728; *Angew. Chem., Int. Ed. Engl.* **1995**, *34*, 1624–1627.
- [42] A. Livoreil, C. Dietrich-Buchecker, J.-P. Sauvage, *J. Am. Chem. Soc.* **1994**, *116*, 9399–9400.
- [43] J.-P. Collin, P. Gaviña, J.-P. Sauvage, *New J. Chem.* **1997**, *21*, 525–528.
- [44] A. Livoreil, J.-P. Sauvage, N. Armaroli, V. Balzani, L. Flamigni, B. Venturi, *J. Am. Chem. Soc.* **1997**, *119*, 12114–12124.
- [45] C. Dietrich-Buchecker, J.-P. Sauvage, J.-P. Kintzinger, *Tetrahedron Lett.* **1983**, *24*, 5095–5098.
- [46] C. Dietrich-Buchecker, J.-P. Sauvage, *Tetrahedron Lett.* **1983**, *24*, 5091–5094.
- [47] C. Dietrich-Buchecker, J.-P. Sauvage, J.-M. Kern, *J. Am. Chem. Soc.* **1984**, *106*, 3043–3045.
- [48] F. Arnaud-Neu, E. Marques, M.-J. Schwing-Weill, C. O. Dietrich-Buchecker, J.-P. Sauvage, J. Weiss, *New J. Chem.* **1988**, *12*, 15–20.
- [49] H. W. Gibson, S.-H. Lee, P. T. Engen, P. Lecavalier, J. Sze, Y. X. Shen, M. Bheda, *J. Org. Chem.* **1993**, *58*, 3748–3756.
- [50] C. Dietrich-Buchecker, J.-P. Sauvage, *Tetrahedron* **1990**, *46*, 503–512.
- [51] C. Dietrich-Buchecker, J.-M. Kern, J.-P. Sauvage, *J. Am. Chem. Soc.* **1989**, *111*, 7791–7800.
- [52] C. Dietrich-Buchecker, P. A. Marnot, J.-P. Sauvage, J.-P. Kintzinger, P. Maltèse, *Nouv. J. Chim.* **1984**, *8*, 573–582.
- [53] P. Federlin, J.-M. Kern, A. Rastegar, C. Dietrich-Buchecker, P. A. Marnot, J.-P. Sauvage, *New J. Chem.* **1990**, *14*, 9–12.
- [54] R. S. Nicholson, I. Shain, *Anal. Chem.* **1964**, *36*, 706–723.

Received: March 29, 1999 [F 1703]